Available online at www.sciencedirect.com
ScienceDirect
Journal of Power Sources 175 (2008) 266–271
JOURNAL OF POWER SOURCES
www.elsevier.com/locate/jpowsour

Short communication

High dispersion and electrocatalytic activity of Pd/titanium dioxide nanotubes catalysts for hydrazine oxidation

Bin Dong [a], Ben-Lin He [a], Jier Huang [b], Guo-Yu Gao [a], Zhi Yang [a], Hu-Lin Li [a,*]

[a] *College of Chemistry and Chemical Engineering of Lanzhou University, Lanzhou 730000, PR China*
[b] *Department of Chemistry, Emory University, Atlanta, GA 30322, USA*

Received 4 July 2007; received in revised form 19 August 2007; accepted 30 August 2007
Available online 4 September 2007

Abstract

Pd/titanium dioxide nanotubes (Pd/TiO_2-NTs) catalysts were prepared by a simple reduction method using TiO_2-NTs as support. The structure and morphology of the resulting Pd/TiO_2-NTs were characterized by transmission electron microscopy and X-ray diffraction. The results showed that Pd nanoparticles with a size range from 6 to 13 nm were well-dispersed on the surface of TiO_2-NTs. The electrocatalytic properties of Pd/TiO_2-NTs catalysts for hydrazine oxidation were also investigated by cyclic voltammetry. Compared to that of pure Pd particles and Pd/TiO_2 particles, Pd/TiO_2-NTs catalyst showed much higher electrochemical activity. This may be attributed to the uniform dispersion of Pd nanoparticles on TiO_2-NTs, smaller particle size and unique properties of TiO_2-NTs support. In addition, the mechanism of hydrazine electrochemical oxidation catalyzed by Pd/TiO_2-NTs are also investigated. The oxidation of hydrazine was an irreversible process, which might be controlled by diffusion process of hydrazine.

Keywords: Titanium dioxide nanotubes; Pd nanoparticles; Supporting materials; Hydrazine oxidation

1. Introduction

The fabrication and electrocatalytic properties of metal catalysts deposited on nanomaterials have been intensely investigated in recent years, motivated by the desire to improve the performance of fuel cells [1–10]. Among many possible combinations of metal catalyst and inert support, palladium (Pd) and palladium group metals-based nanocomposites are one of the most widely employed catalysts for the electrochemical reactions in fuel cells operating with acid or alkaline electrolytes [5,6,8]. Employing inert nanomaterials as catalyst support can potentially introduce the unique properties of support materials, such as high surface area, chemical stability, to metal catalysts, thus increase the efficiency of metal catalysts [11–14]. Suffredini et al. [15] have found that the good electrocatalytic properties for the oxidation of ethanol were obtained on Pt–RuO_2/C electrode. Bai et al. [16] reported that Pt–ZrO_2/C had higher peak current density and lower peak potential than Pt/C. TiO_2-NTs have also been paid significant attention due to their features related to large surface area, non-toxicity, chemical stability and low production cost, which makes them valuable functional materials in many areas [17–19]. The introduction of TiO_2-NTs can also enhance the overall reactivity of the catalytic centers and help to obtain good interaction between the support and metal particles because of the abundant hydroxyl on the surface of TiO_2-NTs [20]. It is also found that certain metal oxides are able to stabilize and disperse adequately a number of active phases and increase CO tolerance based upon the bi-functional mechanism [21] and the electronic effect [22]. All of these show that TiO_2-NTs are ideal choice of supporting materials for high performance catalysts.

TiO_2-NTs have been adopted as chemical catalysts support for water treatment and methanol oxidation [23,24]. And good catalytic results were obtained. Hydrazine ($N_2H_4{\cdot}H_2O$) is an important high-performance fuel in energy storage and conversion for aero and space fields, which also have promising application in fuel cells. However, the oxidation of hydrazine on Pd/TiO_2-NTs catalysts have been seldom reported. So it is very meaningful to study the catalytic mechanisms of hydrazine on Pd/TiO_2-NTs.

* Corresponding author. Tel.: +86 931 891 2517; fax: +86 931 891 2582.
E-mail address: lihl@lzu.edu.cn (H.-L. Li).

0378-7753/$ – see front matter © 2007 Published by Elsevier B.V.
doi:10.1016/j.jpowsour.2007.08.090

In present work, we synthesized well-dispersed Pd nanoparticles catalysts with TiO_2-NTs as supporting materials. The electrocatalytic activity of as-synthesized Pd/TiO_2-NTs for hydrazine oxidation was investigated by cyclic voltammetry (CV). Compared to Pd particles and Pd/TiO_2 particles, Pd/TiO_2-NTs show much higher catalytic activity to electro-oxidation of hydrazine. Additionally, the dependence of the electrocatalytic performance on the properties of Pd/TiO_2-NTs as well as the reaction mechanism of hydrazine oxidation will be discussed.

2. Experimental

2.1. Preparation of TiO_2-NTs

The rutile TiO_2 powders can be converted to anatase TiO_2-NTs through the hydrothermal process. Therefore, the rutile TiO_2 powders synthesized according to our previous work [25] were used to prepare pure anatase TiO_2-NTs by the following hydrothermal process. In a typical synthesis, 100 mg rutile TiO_2 powders were added into a teflon-lined stainless steel autoclave with 10 M NaOH solution (45 ml). The sealed autoclave was heated to 110 °C in 2 h and maintained for 20 h, then cooled to room temperature in air. The obtained TiO_2-NTs were firstly filtered and washed with deionized water for neutral, then dispersed in 0.1 M HNO_3 solution by ultrasonication for 30 mins. The acid-treated TiO_2-NTs were washed continually with deionized water to pH 7. Finally, the samples were dried in vacuum overnight at 80 °C.

FT-IR spectra of TiO_2-NTs used in our work were collected using a Nicolet Nexus 670 Fourier transform infrared spectrometer. The result is shown in Fig. 1. The peak value of hydroxyl groups is at 3350.84 cm^{-1} and the intensity is very strong, which indicates large amount of hydroxyl groups appear on the surface of TiO_2-NTs. And the peak values of 1629.61 and 1337.01 cm^{-1} correspond to TiO_2-NTs. The hydroxyl groups on TiO_2-NTs can help the conjunction and dispersion of metal particles.

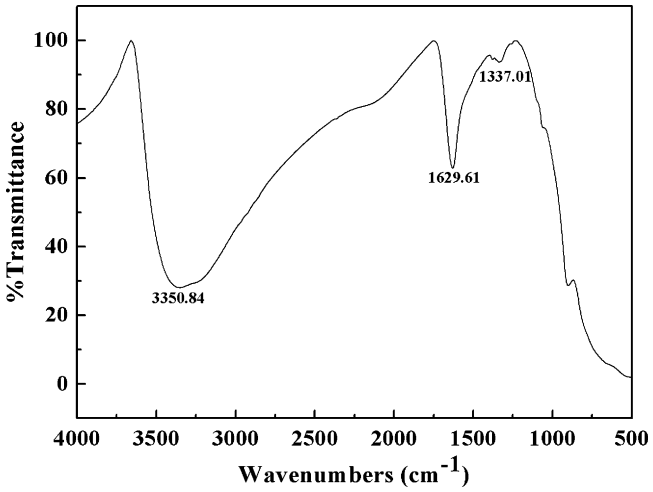

Fig. 1. FT-IR spectra of TiO_2-NTs.

2.2. Preparation of Pd/TiO_2-NTs catalysts

The typical procedure used to prepare Pd/TiO_2-NTs catalysts was shown schematically in Fig. 2. Firstly, the aqueous palladium chloride solution was heated in 50 °C water bath in order to avoid precipitation of palladium black. Then TiO_2-NTs were added to the palladium chloride solution under vigorous stirring. After the solution was stirring for 1 h, which allowed ion exchange between palladium chloride and the protons of hydroxyl on TiO_2-NTs [26]. Formol, as a reducing agent, was added to the system under vigorous stirring. The resulting solution was further stirred for 3 h at 50 °C, followed by washing with deionized water and drying in vacuum at 80 °C for 12 h. In order to study the effect of temperature on the morphology of the catalyst, the reductive reaction was also performed under 20 and 80 °C, respectively. The colors of Pd/TiO_2-NTs catalysts obtained under different temperatures changed from white to orange-brown with the increasing of the temperature. For comparison, Pd/TiO_2 particles and unsupported Pd particles have also been synthesized at 50 °C respectively under the same reaction conditions.

2.3. Characterization of Pd/TiO_2-NTs catalysts

Electrochemical measurements were performed by CHI600 electrochemical workstation (Chenhua, Shanghai) with a conventional three-electrode electrochemical cell. To prepare the working electrode, Pd/TiO_2-NTs catalysts were firstly dispersed in Nafion ethanol solution and sonicated for 5 min. Then the well-mixed catalysts solution was deposited on the surface of the glassy carbon (GC) electrode with the geometric area of 0.07 cm^2. The Pd loading on the electrode was controlled at 0.5 mg cm^{-2}. A platinum foil was served as counter electrode and a saturated calomel electrode (SCE) was used as reference electrode. All potentials were measured and reported with respect to SCE in this paper. CV scans were recorded from 0 to

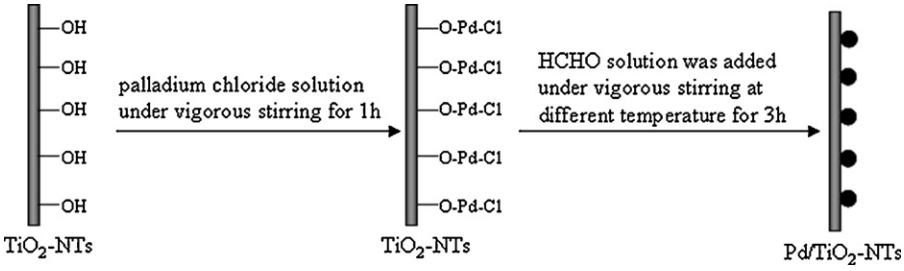

Fig. 2. A schematic diagram showing the steps for the synthesis of Pd/TiO_2-NTs catalysts.

0.6 V. For the exact comparison, all CV curves in our work are collected under steady-state conditions.

The structure of TiO_2-NTs and Pd/TiO_2-NTs catalysts was characterized by X-ray diffraction (XRD) using a Rigaku/DMAX 2400 diffractometer (Japan) with Cu Ka radiation ($\lambda = 1.54178$ Å) monochromated radiation operating at 40.0 kV and 60.0 mA. XRD data were collected in the 2θ ranges from 10° to 90°.

Transmission electron microscope (TEM, Hitachi 600, Japan) was used to examine the morphology of the samples. The samples were prepared by dropping the ethanol solution of TiO_2-NTs and Pd/TiO_2-NTs catalysts on the Cu grids and were observed at 100 kV.

3. Results and discussion

3.1. TEM analysis of TiO_2-NTs and Pd/TiO_2-NTs catalysts

The TEM images of TiO_2-NTs are shown in Fig. 3. It can be seen that TiO_2-NTs are made of mutilayered sheets with the outer diameter in the range of 10–15 nm. The mechanisms for the formation of TiO_2-NTs may be as follows: firstly, Ti–O–Na bonds exist on the surface of TiO_2 owing to the action of NaOH. When the samples are treated with distilled water, Ti–O–Na bond is gradually converted into a Ti–OH bond which may form a sheet on TiO_2 surface. After the sample is treated by acid, the Ti–O–Ti bonds or Ti–O–H···O–Ti hydrogen bonds are generated. This significantly decreases bond distance between Ti–O, thus leads to the folding of the sheet to a tube structure [20].

The direct evidence of the formation of Pd nanoparticles on the surface of TiO_2-NTs is given by Fig. 4. It can be seen from Fig. 4b that Pd nanoparticles on TiO_2-NTs surface reduced at 50 °C are spherical and slightly flattened with sizes in the range of 6–13 nm. Compared to the particles reduced at 20 and 80 °C, Pd particles on TiO_2-NTs synthesized at 50 °C are more uniform. At 20 °C only small amounts of Pd particles exist on TiO_2-NTs, while obvious aggregation of Pd particles on TiO_2-NTs are observed at 80 °C. The non-uniform dispersion of Pd particles on TiO_2-NTs may be generally attributed to many factors such as the stucture and surface energy of supporting materials, the rapid reaction, vigorous stirring and slow addition of reducing agent [27–29]. In our work, the reductive reaction may not be complete at low temperature (20 °C) and thus few Pd particles were anchored onto TiO_2-NTs. However, at high temperature (80 °C) the reaction rate is so fast that leads to the aggregation of Pd particles on TiO_2-NTs, which might reduce the active points of metal catalysts. Therefore, controlling the temperature of reductive reaction at 50 °C can help to get good dispersion of Pd particles and more catalytic active particles on the surface of TiO_2-NTs. Higher electrocatalytic activity of Pd/TiO_2-NTs catalysts synthesized at 50 °C might be expected.

3.2. XRD pattern of TiO_2-NTs and Pd/TiO_2-NTs catalysts

The typical powder XRD patterns of TiO_2-NTs and Pd/TiO_2-NTs catalysts are shown in Fig. 5a and b, respectively. All

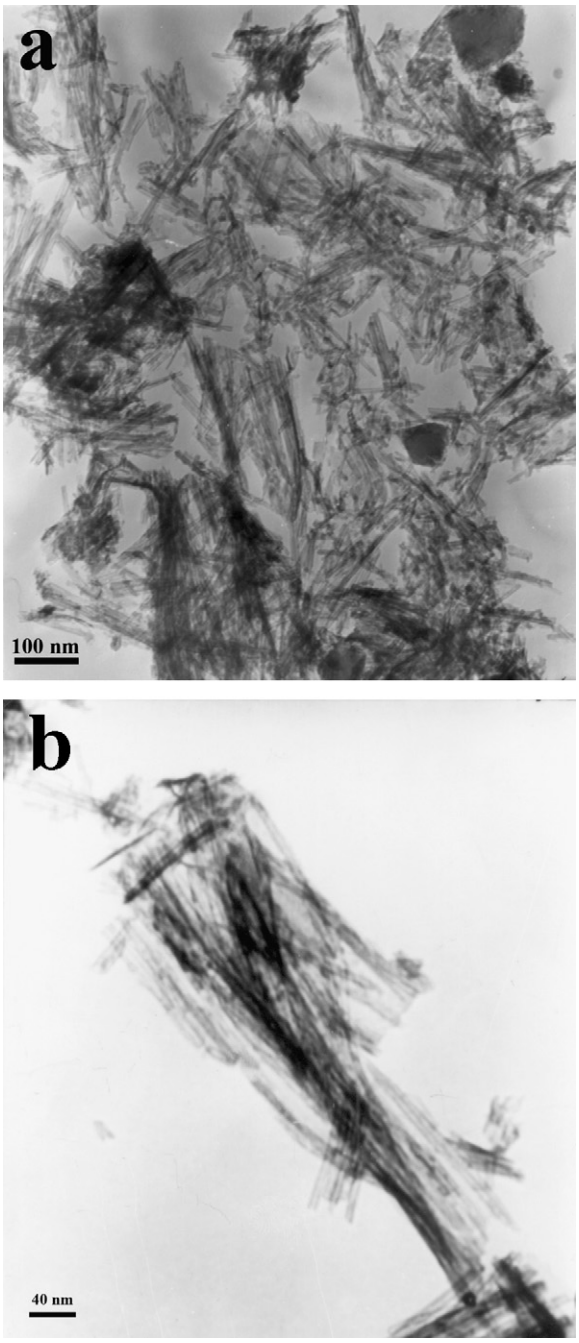

Fig. 3. The TEM images of TiO_2-NTs with low magnification (a) and with high magnification (b).

peaks of Fig. 5a can be indexed to pure anatase TiO_2, which is in good agreement with the standard spectrum (JCPDS, card no.: 21-1272). The diffraction planes of anatase (Fig. 5a) are sharp indicating good crystallization of TiO_2-NTs. As shown in Fig. 5b, all diffraction peaks of TiO_2-NTs are observed. Actually, other three peaks have the same positions in the *X*-axis in Fig. 5a (47.12°, 68.65° and 82.47° assigned to (2 0 0), (2 2 0) and (3 1 1) reflection of Pd, which were coincided well with the diffraction (2 0 0), (1 1 6) and (2 2 4) planes of anatase TiO_2, respectively). Furthermore, the major diffraction peaks of Pd nanoparticles can also be clearly observed. The peaks at 40.40° can be assigned to

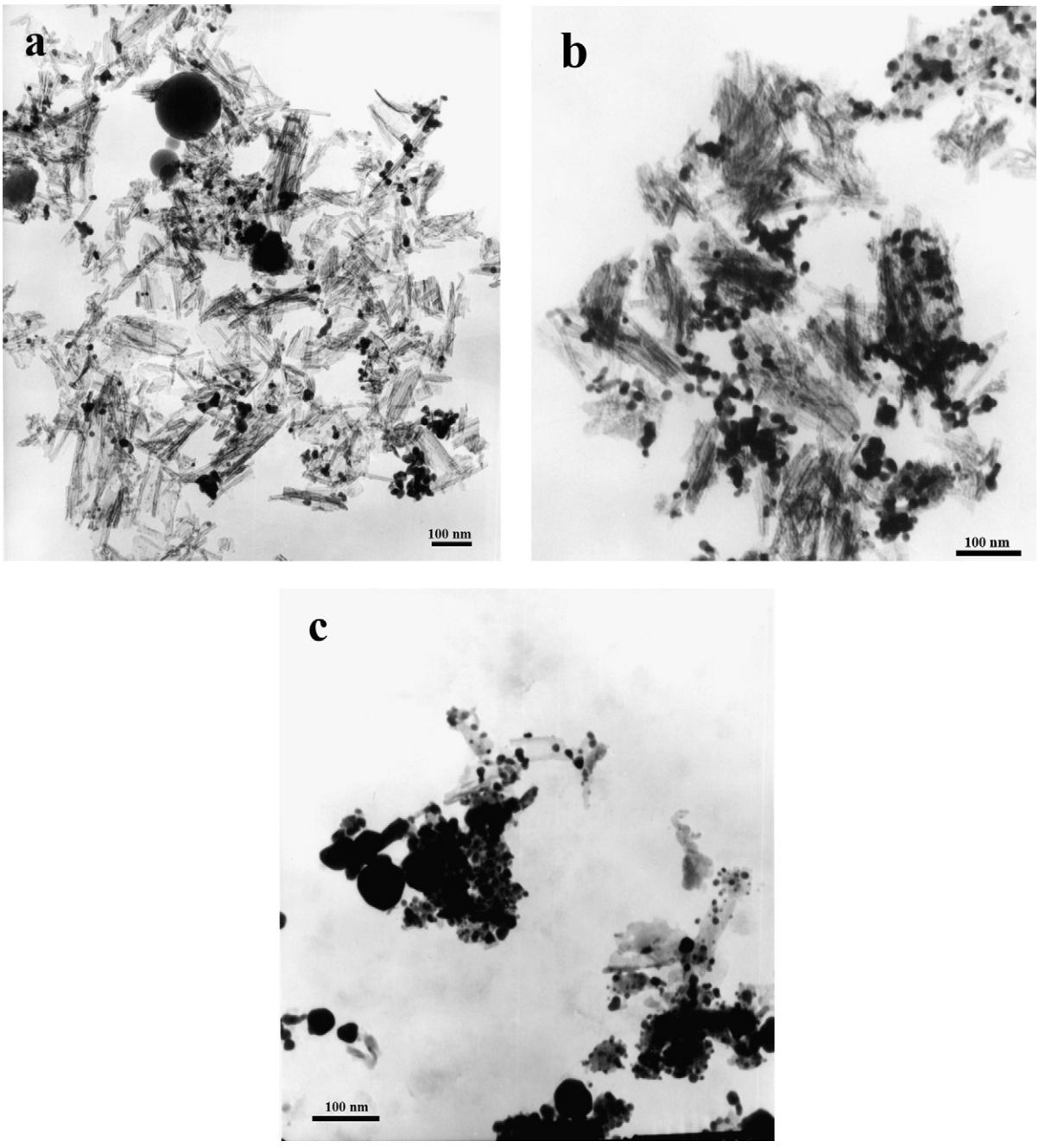

Fig. 4. The TEM images of Pd/TiO_2-NTs synthesized at different temperatures: (a) 20 °C, (b) 50 °C and (c) 80 °C.

(1 1 1) reflection of Pd, which are a little broad due to the small size of Pd nanoparticles.

3.3. Electrochemical performance of Pd/TiO_2-NTs catalysts

The electro-oxidation of hydrazine was performed on GC electrode modified with all kinds of Pd catalysts by CV. Fig. 6 shows the CV curves of pure TiO_2-NTs, Pd/TiO_2 particles, unsupported Pd and Pd/TiO_2-NTs synthesized at 50 °C in solution of 10 mM $N_2H_4{\cdot}H_2O$ in 0.1 M K_2SO_4. It is clear that hydrazine cannot be electro-oxidized on pure TiO_2-NTs modified GC electrode, whereas for Pd/TiO_2-NTs, hydrazine is electro-oxidized at 0.323 V with the current of 3.6 mA cm^{-2}, which is in good agreement with literature reports [30,31]. No peak appears on the negative potential scan, which implies that the electro-oxidation of hydrazine may be an irreversible process. However, for Pd/TiO_2 particles and unsupported Pd, the hydrazine is able to be electro-oxidized at more positive potential with smaller current, which indicates that the two catalysts have worse catalytic activity than Pd/TiO_2-NTs. The reason may be that the dispersion and size of Pd particles are different among the three catalysts. The TiO_2-NTs have larger surface area than TiO_2 particles and therefore Pd nanoparticles can better disperse on the surface of TiO_2-

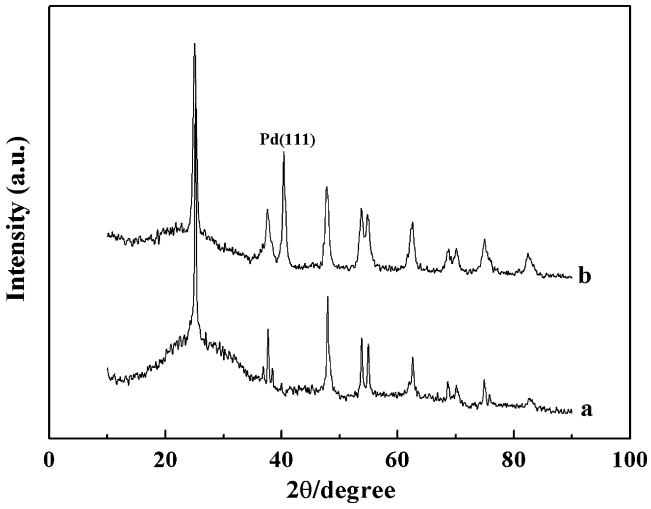

Fig. 5. XRD patterns for TiO_2-NTs (a) and Pd/TiO_2-NTs catalysts (b).

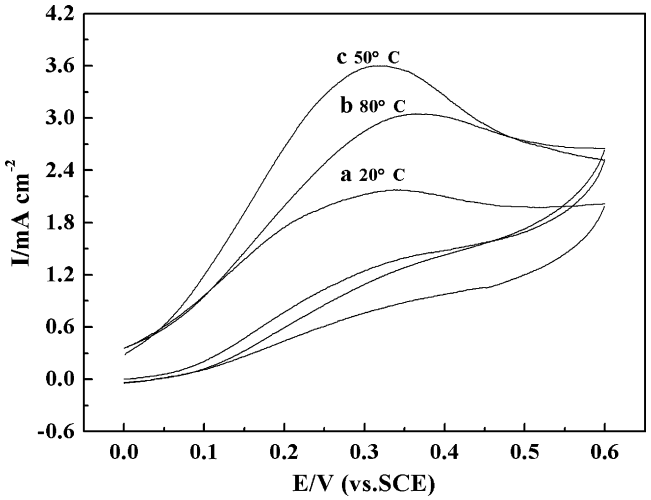

Fig. 7. Cyclic voltammograms of 10 mM $N_2H_4{\cdot}H_2O$ in 0.1 M K_2SO_4 solution at Pd/TiO_2-NTs electrode synthesized at different temperatures: (a) 20 °C, (b) 50 °C and (c) 80 °C. Scan rate: 50 mV s^{-1}.

NTs. The unsupported Pd particles synthesized have larger size and more aggregation than Pd nanoparticles on the supporting materials, which results into fewer catalytic activity points.

The CV curves of electro-oxidation of hydrazine catalyzed by Pd/TiO_2-NTs synthesized at different temperatures 20 °C (curve a), 80 °C (curve b), 50 °C (curve c) are shown in Fig. 7. Significant difference at hydrazine oxidation potential and peak current are observed. Pd/TiO_2-NTs synthesized at 50 °C show the most negative oxidation potential and the highest peak current, which imply that the samples at 50 °C have better catalytic activity for hydrazine electro-oxidation. This is consistent with the results of TEM. The reasons can be concluded as following: the palladium chloride may not be reduced completely at 20 °C and only few amounts of Pd nanoparticles are formed on TiO_2-NTs, which results bad catalytic effect. However, the much rapid reaction rate at 80 °C easily causes aggregation of Pd nanoparticles on the surface of TiO_2-NTs, which reduces the amounts of catalytic activity points exposed on the surface of the electrode. Hence, the further electrochemistry measurement will be carried out on the electrode modified with Pd/TiO_2-NTs synthesized at 50 °C.

Fig. 8 shows CV curves of 10 mM $N_2H_4{\cdot}H_2O$ in 0.1 M K_2SO_4 solution at Pd/TiO_2-NTs (50 °C) electrode at different scan rate (ν) 30, 50, 70, 100, 150 mV s^{-1}. It can be seen that the oxidation potential and peak current for hydrazine oxidation become larger with the increasing of scan rate. Fig. 9 is a dependence curve of the peak currents on the square root of scan rates. The linear relationship is observed. It can be concluded that the electrocatalytic oxidation hydrazine on Pd/TiO_2-NTs may be controlled by a diffusion process [30,32].

The peak potential (E_p) increases with increased of ν, and a linear relationship can be obtained between E_p and log(ν), as shown in Fig. 10. This linear relationship is similar with the previous report [30], indicating that the oxidation of hydrazine is an irreversible electrode process. The electron transfer numbers

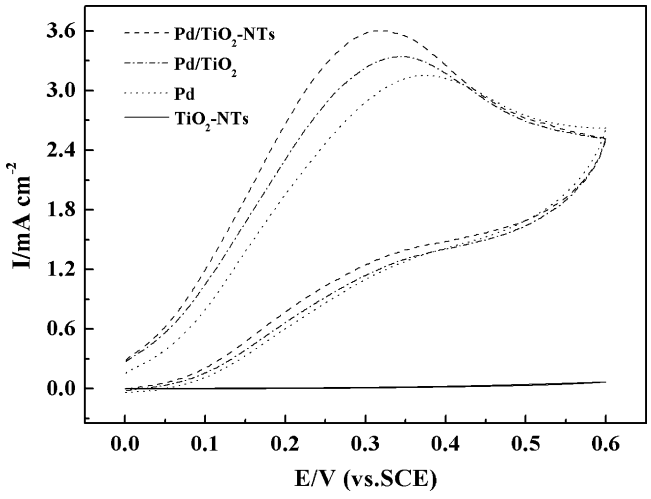

Fig. 6. Cyclic voltammograms of 10 mM $N_2H_4{\cdot}H_2O$ in 0.1 M K_2SO_4 solution at TiO_2-NTs, Pd/TiO_2, unsupported Pd and Pd/TiO_2-NTs electrode. Scan rate: 50 mV s^{-1}.

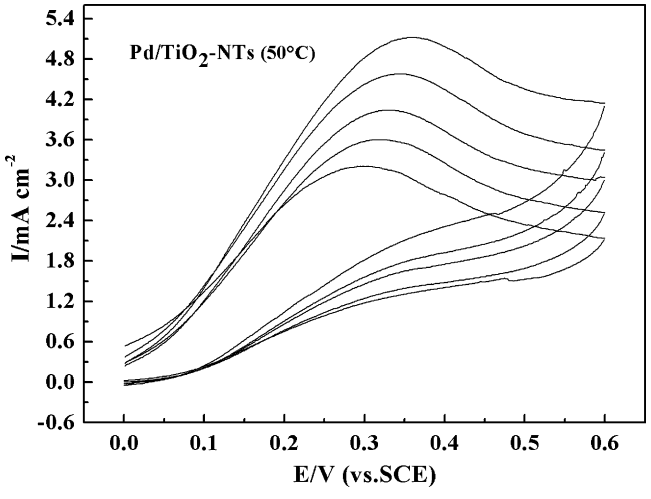

Fig. 8. Cyclic voltammograms of 10 mM $N_2H_4{\cdot}H_2O$ in 0.1 M K_2SO_4 solution at Pd/TiO_2-NTs (50 °C) electrode (scan rate: 30, 50, 70, 100, 150 mV s^{-1} from inner to outer).

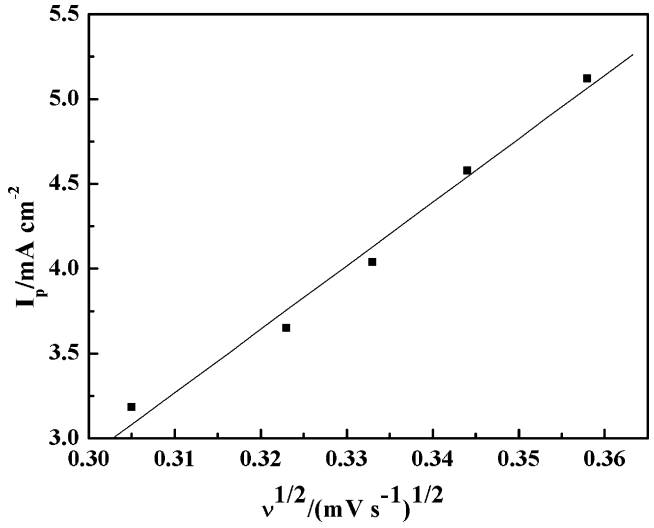

Fig. 9. I_p vs. $\nu^{1/2}$ plot of cyclic voltammograms of Pd/TiO_2-NTs (50 °C) electrode (scan rate: 30, 50, 70, 100, 150 mV s^{-1}).

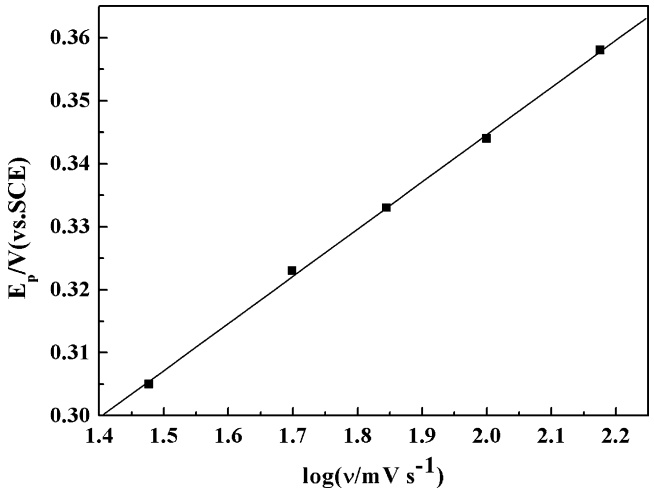

Fig. 10. E_p vs. log ν plot of cyclic voltammograms of Pd/TiO_2-NTs (50 °C) electrode (scan rate: 30, 50, 70, 100, 150 mV s^{-1}).

$n = 4$ can be calculated, and the overall oxidation reaction of hydrazine can be written as $NH_2NH_3^+ \rightarrow N_2 + 5H^+ + 4e$ [30]. The high stability of N_2 molecule explains why no peak appeared on the negative potential scan.

4. Conclusion

In this work, Pd/TiO_2-NTs catalysts with high activity are successfully prepared by simple reduction method. TEM images reveal that the well-dispersed, spherical Pd nanoparticles are anchored onto TiO_2-NTs, which may be attributed to excellent structure and reactive hydroxyl of TiO_2-NTs. The cyclic voltammetry measurements for hydrazine oxidation showed that Pd/TiO_2-NTs have better catalytic activity than Pd/TiO_2 particles and unsupported Pd particles. Further study show that hydrazine oxidation catalyzed by Pd/TiO_2-NTs is an irreversible process, which might be controlled by diffusion process of hydrazine. These results imply that TiO_2-NTs are one of most promising supporting materials for noble metals catalysts.

Acknowledgement

This work is supported by the National Natural Science Foundation of China (NNSFC 60471014).

References

[1] E.S. Steigerwalt, G.A. Deluga, C.M. Lukehart, J. Phys. Chem. B 106 (2002) 760–766.
[2] D.A. Stevens, S. Zhang, Z. Chen, J.R. Dahn, Carbon 41 (2003) 2769–2777.
[3] J.T. Moore, D. Chu, R.Z. Jiang, G.A. Deluga, C.M. Lukehart, Chem. Mater. 15 (2003) 1119–1124.
[4] X. Sun, R. Li, D. Villers, J.P. Dodelet, S. Desilets, Chem. Phys. Lett. 379 (2003) 99–104.
[5] C. Rice, S. Ha, R.I. Masel, A. Wieckowski, J. Power Sources 115 (2003) 229–235.
[6] T. Okada, N. Arimura, C. Ono, M. Yuasa, Electrochim. Acta 51 (2005) 1130–1139.
[7] D.J. Guo, H.L. Li, J. Power Sources 160 (2006) 44–49.
[8] P.K. Shen, C.W. Xu, Electrochem. Commun. 8 (2006) 184–188.
[9] T. Onoe, S. Iwamoto, M. Inoue, Catal. Commun. 8 (2007) 701–706.
[10] J. Solla-Gull, E. Lafuente, A. Aldaz, M.T. Martinez, J.M. Feliu, Electrochim. Acta 52 (2007) 5582–5590.
[11] V. Lordi, N. Yao, J. Wei, Chem. Mater. 13 (2001) 733–735.
[12] J.S. Yu, S. Kang, S.B. Yoon, G. Chai, J. Am. Chem. Soc. 124 (2002) 9382–9383.
[13] K.Y. Chan, J. Ding, J. Ren, S. Cheng, K.Y. Tsang, J. Mater. Chem. 14 (2004) 505–516.
[14] J. Guzman, S. Carrettin, A. Corma, J. Am. Chem. Soc. 127 (2005) 3286–3287.
[15] H.B. Suffredini, V. Tricoli, L.A. Avaca, N. Vatistas, Electrochem. Commun. 6 (2004) 1025–1028.
[16] Y.X. Bai, J.J. Wu, J.Y. Xi, J.Sh. Wang, W.T. Zhu, L.Q. Chen, X.P. Qiu, Electrochem. Commun. 7 (2005) 1087–1090.
[17] A.R. Armstrong, G. Armstrong, J. Canales, P.G. Bruce, Angew. Chem. Int. Ed. 43 (2004) 2286–2288.
[18] J. Li, L. Li, L. Zheng, Y. Xian, L. Jin, Talanta 68 (2006) 765–770.
[19] A.Y.H. Lo, R.W. Schurko, M. Vettraino, B.O. Skadtchenko, M. Trudeau, D.M. Antonelli, Inorg. Chem. 45 (2006) 1828–1838.
[20] T. Kasuga, M. Hiramatsu, A. Hoson, T. Sekino, K. Niihara, Adv. Mater. 11 (1999) 1307–1311.
[21] J.M. Leger, S. Rousseau, C. Coutanceau, F. Hahn, C. Lamy, Electrochim. Acta 50 (2005) 5118–5125.
[22] C. Lu, C. Rice, R.I. Masel, P.K. Babu, P. Waszczuk, H.S. Kim, E. Oldfield, A. Wieckowski, J. Phys. Chem. B 106 (2002) 9581–9589.
[23] T. Garcia, B. Solsona, S.H. Taylor, Catal. Lett. 97 (2004) 99–103.
[24] M. Wang, D.J. Guo, H.L. Li, J. Solid State Chem. 178 (2005) 1996–2000.
[25] Y.K. Zhou, L. Cao, F.B. Zhang, B.L. He, H.L. Li, J. Electrochem. Soc. 150 (9) (2003) A1246–A1249.
[26] L. Torrente-Murciano, A.A. Lapkina, D.V. Bavykin, F.C. Walsh, K. Wilson, J. Catal. 245 (2007) 272–278.
[27] G. Wu, Y.S. Chen, B.Q. Xu, Electrochem. Commun. 7 (2005) 1237–1243.
[28] D.V. Bavykin, A.A. Lapkin, P.K. Plucinski, L. Torrente-Murciano, J.M. Friedrich, F.C. Walsh, Top. Catal. 39 (2006) 151–160.
[29] K.F. Zhang, D.J. Guo, X. Liu, J. Li, H.L. Li, Z.X. Su, J. Power Sources 162 (2006) 1077–1081.
[30] D.J. Guo, H.L. Li, J. Colloid Interface Sci. 286 (2005) 274–279.
[31] C. Batchelor-McAuley, C.E. Banks, A.O. Simm, T.G.J. Jones, R.G. Compton, Analyst 131 (2006) 106–110.
[32] K. Honda, M. Yoshimura, T.N. Rao, D.A. Tryk, A. Fujishima, J. Electroanal. Chem. 514 (2001) 35–50.